CHEMISTRY
A EUROPEAN JOURNAL

DOI: 10.1002/chem.200701919

Iron Chelates of 2,2′-Bidipyrrin: Stable Analogues of the Labile Iron Bilins

Martin Bröring,*[a] Silke Köhler,[a] Stephan Link,[a] Olaf Burghaus,[a] Clemens Pietzonka,[a] Harald Kelm,[b] and Hans-Jörg Krüger[b]

Abstract: A unique series of halogenidoiron(III) complexes of the open-chain tetrapyrrolic ligand 2,2′-bidipyrrin (bpd) ([FeX(bdp)] X = F, Cl, Br, I) was prepared from simple pyrrolic and bipyrrolic precursors and iron chloride by a one-pot condensation/metalation strategy, followed by salt metathesis with CsF, LiBr, or NaI. Crystallographic analysis revealed that in all cases the 2,2′-bidipyrrin ligand is forced to reside in a helical conformation when bound to the iron atom. Whereas the extremely sensitive fluorido derivative was isolated as a CsF adduct and forms 1D polymeric chains in the solid state, the more stable chlorido, bromido, and iodido derivatives crystallize as discrete monomeric molecules with a distorted pentacoordinate iron(III) ion in an intermediate spin ground state. Magnetic susceptibility measurements and Mössbauer data of the compounds are in agreement with this interpretation. In solution, however, all the compounds are pentacoordinate with the iron atom in the high-spin ($S = 5/2$) state and dynamic with respect to helix inversion. In the presence of air, the iron chelates react stepwise with the nucleophiles methanol and imidazolate at the tetrapyrrole terminal α,ω-positions, presumably through the hexacoordinate species $[Fe(bdp)(MeOH)_2]^+$ and $[Fe(im)_2(bdp)]^-$, respectively. The successive increase of strain at these positions results in increasingly labile intermediates that spontaneously release the iron ion from the mono- or disubstituted tetrapyrrole ligands.

Keywords: bilins · helicity · heme degradation · iron · porphyrinoids

Introduction

Heme oxygenase (HO) constitutes a much studied and ubiquitous enzyme class active in biological heme degradation.[1] HO cleaves the porphyrin macrocycle of iron protoporphyrin IX in a multistep redox reaction regiospecifically at the α position.[2] The iron(III) complex of biliverdin IXα (BV-IXα), which is usually designated as the primary product of HO action, irreversibly releases the iron ion first after a one-electron reduction as iron(II), followed by the free-base biliverdin.[3–5] Nature uses the iron ion and carbon monoxide, released in this complicated transformation from heme to BV-IXα, for a number of different functions. In cyanobacteria and higher plants, BV-IXα is the general precursor for several essential light-harvesting pigments, while iron reutilization and cellular signaling are major functions of HO in mammals. Some bacterial pathogens express HO to acquire iron by breaking down the heme of their host. Earlier attempts to prepare iron complexes of BV-IXα or related bilin model ligands in vitro have either failed or led to unsatisfactory results.[6–9] The reported observations, therefore, support the biologically important lability and the distinct inclination of such complexes to lose the iron ion spontaneously.

In 2004, the first stable iron biliverdin model **1** was reported (Scheme 1).[10] The well-characterized **1** forms during an oxidative ring-opening reaction from a verdoheme precursor and constitutes a one-electron oxidized model of the naturally occurring complex. To the best of our knowledge, **1** is so far the only exception from the rule that iron complexes of open-chain tetrapyrrolic ligands are too reactive to be investigated in more detail. The situation is special for iron, as similar complexes of other 3d transition metals, such as Zn, Cu, Ni, Co, or Mn, are more readily available and relatively stable (though still reactive) in solution.[11–25]

[a] Prof. Dr. M. Bröring, Dr. S. Köhler, Dr. S. Link, Dr. O. Burghaus, C. Pietzonka
Fachbereich Chemie
Philipps-Universität Marburg
Hans-Meerwein-Strasse, 35043 Marburg (Germany)
Fax: (+49) 6421-282-5653
E-mail: Martin.Broering@chemie.uni-marburg.de

[b] Dr. H. Kelm, Prof. H.-J. Krüger
Fachbereich Chemie
Universität Kaiserslautern
Erwin-Schrödinger Strasse, 67663 Kaiserslautern (Germany)

Supporting information for this article is available on the WWW under http://www.chemeurj.org/ or from the author.

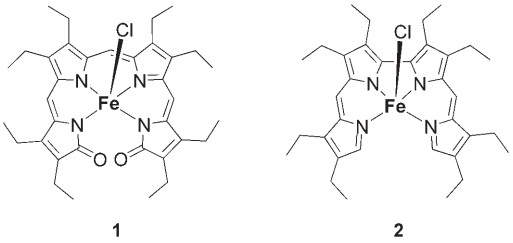

Scheme 1. Iron bilindione **1**[10] and [FeCl(bdp)] (**2**).

To study the decomposition process of an intrinsically unstable species, a stable model compound is required that can be chemically modified in such a way that the lability increases. We assumed that the intramolecular repulsion of the oxygen termini of bilindione compounds adds significantly to the observed lability of FeBV-IXα and its models. For a more stable model compound, we have, thus, thought to remove the central CH bridge and exchange the oxygen for hydrogen atoms. By implementing these measures, we designed the preparatively readily accessible 2,2′-bidipyrrin (H_2(bdp)) with two reactive termini.[26–28] A substitution of hydrogen atoms for any other group at these positions would directly enhance the intramolecular repulsion and, therefore, the lability in complexes of such tetrapyrroles. 2,2′-Bidipyrrin compounds have been explored before as nitrogen-containing ligands in a number of mono- and dinuclear transition-metal chelates,[17,20,22,24,25,29,30] and the propensity of the terminal positions for chemical transformations has occasionally been documented.[31–34] Stable iron chelates, such as **2**, can indeed be obtained from these ligands (Scheme 1), and we report herein the preparation, structure, spectroscopic analysis, and biomimetic reactivity of a unique series of iron 2,2′-bidipyrrin complexes [FeX(bdp)] (X = F, Cl, Br, I).

Results and Discussion

Synthesis and analytical results of [FeX(bdp)] complexes 2 and 5–7: All initial attempts to prepare iron chelate complexes of 2,2′-bidipyrrin ligands by the reaction of the latter with simple iron(II) or iron(III) precursors failed for unclear reasons and did not yield a trace of product. In general, no reaction could be observed at all during these attempts except for an unspecific decomposition of the tetrapyrrole, which was observed over largely extended reaction times. The synthesis of the chloride complex **2** was finally achieved accidentally by a multistep one-pot reaction comprising initial condensation of dialdehyde **3** and pyrrole **4** with $POCl_3$, followed by basification with triethylamine and metalation using a $FeCl_2$/$FeCl_3$ mixture in ethereal solution under aerobic conditions. A dark residue was obtained after suitable aqueous work-up, and repeated crystallization from *n*-hexane yielded the title compound as a dark powder with a metallic sheen in a reproduced yield of 42% (Scheme 2). Further investigations revealed that the in situ preparation

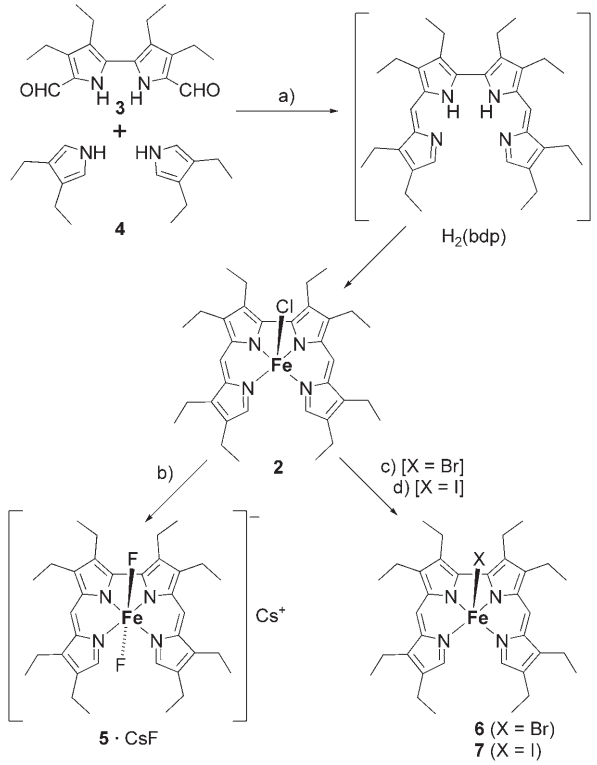

Scheme 2. Preparation of [FeCl(bdp)] (**2**) from simple pyrrolic precursors **3** and **4**, and salt metathesis to yield products **5**–**7**. a) CH_2Cl_2, $POCl_3$, then NEt_3, dioxane, $FeCl_2{\cdot}4H_2O$, $FeCl_3$ (42%); b) CsF, CH_2Cl_2, 2-propanol (19%); c) LiBr, CH_2Cl_2, 2-propanol (94%); d) NaI, acetone (80%).

of the bidipyrrin ligand, the addition of the preformed ligand to the metal precursor solution (and not vice versa) immediately after basification, the exact amount of excess triethylamine used in this step, and the presence of iron ions in both the +2 and +3 oxidation states are essential for the formation of the product. In addition, the choice of the solvent (dioxane versus THF) is critical for the isolation of sufficiently pure material from the reaction mixture. Several recrystallization processes finally produced **2** in analytical purity.

As a result of the sensitivity of **2** in solution, the exchange of the chloride ligand against another halide ligand poses a special challenge and requires the application of optimized protocols for each case. The best reagents for this issue are the organosoluble salts CsF, LiBr, and NaI, which cleanly yield the desired complexes **5**–**7** upon treatment in large excess. The fluoride derivative **5** is too labile for aqueous work-up but can be crystallized directly from the reaction mixture as a CsF adduct. Except for the extremely sensitive **5**, all new complexes gave correct combustion analyses. Additional analysis of **2**, **5**, and **6** by high-resolution mass spectrometry (HRMS) confirmed the presence of one (**2**, **6**) or two halide ligands (**5**; detected in negative-ion mode). For the iodido derivative **7**, however, only the $[Fe(bdp)]^+$ fragment could be identified with this method.

Solid-state properties: The complexes [FeCl(bdp)] (**2**), [FeBr(bdp)] (**6**), and [FeI(bdp)] (**7**) form well-developed crystals by slow evaporation of solutions of dichloromethane/*n*-hexane. Complexes **6** and **7** crystallize isomorphously in the triclinic system, whereas the chlorido derivative **2** displays a different packing pattern and orders in a monoclinic system. None of the crystals contain solvent molecules. Details of the X-ray diffraction studies are given in Table 1. Figure 1 and Figure 2 summarize the molecular structures of **2**, **6**, and **7**.

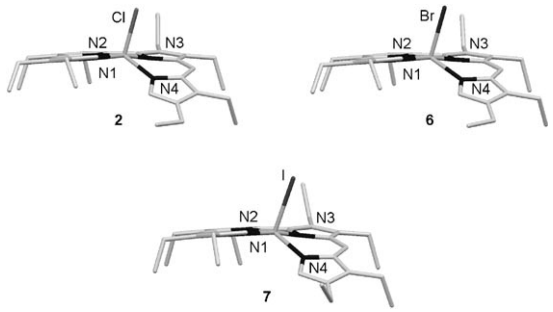

Figure 1. Molecular structures of [FeCl(bdp)] (**2**), [FeBr(bdp)] (**6**), and [FeI(bdp)] (**7**): views of the uneven helical distortion of the tetrapyrrolic ligands.

Despite the differences in the packing pattern, the molecular structures of **2**, **6**, and **7** are very similar and not significantly altered by any sort of packing effect. The special metrics and conformation of these molecules will be explained

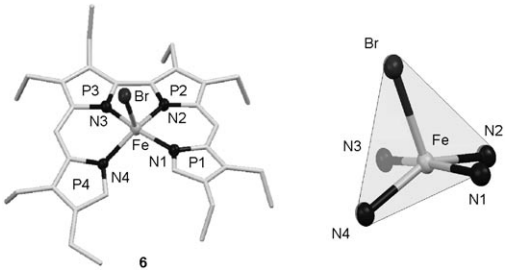

Figure 2. Molecular structure of [FeBr(bdp)] (**6**) with assignment of the {C_4N} planes (left, P1–P4) and view of the distorted trigonal-bipyramidal coordination polyhedron of the iron center (right).

by the structure of **6**. For the sake of comparison, the molecular data for **2**, **6**, and **7** are summarized in Table 2. The results from the X-ray crystallographic analysis of **6** reveal the presence of mononuclear entities in the solid state. The coordination of the iron atom in **6** is best described as distorted trigonal bipyramidal with N1 and N3 in axial positions and N2, N4, and Br in equatorial positions. The Fe–N bond lengths of 1.885–1.981 Å are shorter than those of halogenidoiron–porphyrinoids (1.99–2.07 Å),[35,36] with the equatorial bonds of each of the chemically equivalent pairs N1,N4 and N2,N3 being noticeably longer than the axial counterparts. In addition, the bromido ligand is bound to the iron atom at a distance of 2.4623 Å, which is larger than typically observed for iron–porphyrinoid complexes (2.33–2.41 Å). The same tendency is apparent for the chlorido and iodido derivatives, which show Fe–X bond lengths of 2.3093 and

Table 1. Crystal data and structure refinement of [FeX(bdp)] complexes **2** and **5**–**7** and for substituted 2,2′-bidipyrrins **10** and **12**.

	2	**5**·CsF	**6**	**7**	**10**	**12**
formula	$C_{34}H_{44}ClFeN_4$	$C_{38.64}H_{53.93}Cl_{7.36}Cs\ F_2FeN_4O_{0.32}$	$C_{34}H_{44}BrFeN_4$	$C_{34}H_{44}IFeN_4$	$C_{36}H_{50}N_4O_2$	$C_{40}H_{50}N_8$
M_r	600.03	1067.24	644.49	691.48	570.80	642.88
crystal system	monoclinic	triclinic	triclinic	triclinic	triclinic	triclinic
space group	$C2/c$	$P\bar{1}$	$P\bar{1}$	$P\bar{1}$	$P\bar{1}$	$P\bar{1}$
a [Å]	26.094(5)	8.398(3)	9.571(1)	9.6743(12)	4.7642(8)	8.791(9)
b [Å]	10.135(5)	13.334(4)	12.764(2)	12.6755(17)	13.025(2)	11.162(9)
c [Å]	24.501(5)	22.276(7)	13.828(2)	14.1221(16)	13.045(3)	18.593(16)
α [°]	90	94.13(3)	94.097(14)	94.690(15)	88.29(2)	74.26(10)
β [°]	99.749(5)	97.72(2)	106.215(14)	104.053(14)	87.61(2)	9.97(11)
γ [°]	90	105.65(2)	98.408(14)	99.440(15)	87.65(2)	85.37(10)
Z	8	2	2	2	1	2
ρ_{calcd} [g cm^{-3}]	1.248	1.507	1.343	1.397	1.173	1.220
radiation	$Mo_{K\alpha}$	$Mo_{K\alpha}$	$Mo_{K\alpha}$	$Mo_{K\alpha}$	$Mo_{K\alpha}$	$Mo_{K\alpha}$
T [K]	193(2)	193(2)	193(2)	193(2)	193(2)	193(2)
Θ range [°]	2.11–26.06	2.31–25.44	2.11–26.14	2.08–26.06	2.18–26.01	1.90–26.05
measured reflections	31269	22253	15925	16506	7914	17281
independent reflections[a]	3732	5886	4050	4120	1639	6378
absorption coefficients	0.584	1.536	1.756	1.426	0.073	0.074
structure solution[b]	direct	direct	direct	Patterson	direct	direct
$R1$[c]	0.0889	0.0603	0.0613	0.0665	0.0499	0.0599
w$R2$[d]	0.1308	0.1680	0.0814	0.0874	0.1201	0.1730

[a] $I > 2\sigma(I)$. [b] All structures were solved using SHELXS Program for Crystal Structure Determination[87] and refined with SHELXL Program for Crystal Structure Refinement.[88] [c] $R1 = \Sigma||F_o| - |F_c||/\Sigma|F_o|$. [d] $wR2 = \{\Sigma[w(F_o^2 - F_c^2)^2]/\Sigma[w(F_o^2)^2]\}^{1/2}$.

Table 2. Selected bond lengths [Å] and angles [°] for **2**, **6**, and **7**.

	2	**6**	**7**
Fe–N1	1.947(3)	1.940(3)	1.942(4)
Fe–N2	1.897(3)	1.893(3)	1.894(3)
Fe–N3	1.896(3)	1.885(3)	1.884(3)
Fe–N4	1.978(3)	1.981(3)	1.967(3)
Fe–X	2.3093(12)	2.4623(6)	2.6686(8)
N1-Fe-N2	89.68(11)	89.96(11)	90.16(14)
N1-Fe-N3	166.26(11)	167.45(11)	168.05(15)
N1-Fe-N4	97.79(11)	97.72(11)	97.75(14)
N1-Fe-X	95.11(8)	94.33(7)	94.61(11)
N2-Fe-N3	79.31(12)	79.69(11)	79.93(14)
N2-Fe-N4	145.37(12)	145.01(10)	147.32(14)
N2-Fe-X	110.04(8)	113.04(7)	110.46(10)
N3-Fe-N4	86.97(12)	87.01(11)	87.30(13)
N3-Fe-X	96.37(9)	96.24(8)	95.11(11)
N4-Fe-X	102.93(8)	100.40(8)	100.49(11)
∢P1–P2[a]	3.77	1.45	1.64
∢P2–P3[a]	8.74	14.43	13.32
∢P3–P4[a]	24.44	22.80	20.99

[a] P1–P4 designate the mean-square planes of the $\{C_4N\}$ rings at N1–N4.

2.6686 Å, respectively, compared to 2.19–2.25 and 2.55–2.62 Å for analogous porphyrinoids. The Fe–N and Fe–Cl bond lengths observed for **2** are, however, similar to those reported for the chloridoiron complex of tetraazaporphyrin,[37] which is reported to contain a $S=3/2$ iron(III) ion in square-pyramidal coordination, and the bond lengths of the coordination polyhedron of the iodido derivative **7** are reminiscent of those found for an iodido iron porphycene in a $S=3/2$ spin state with a tiny amount of $S=5/2$ admixture.[36]

The characteristic helicity and the intramolecular strain of metal chelates of open-chain tetrapyrroles is clearly present in **6**, as quantified by the dihedral angle N1-N2-N3-N4 of 18.42°, albeit less pronounced than in the known pentacoordinate chloridoiron complex **1** of the oxidized α,ω-dioxobilin ligand (26.43°).[10] A striking feature of the ligand conformation in all three molecules is the fact that one dipyrrin subunit P1,P2 is almost planar, while the other two $\{C_4N\}$ rings are increasingly bent away from this plane. This observation can be quantified by the dihedral angles between the mean-square planes of the four pyrrole rings P1–P4, which develop from P1–P2 1.45° over P2–P3 14.43° to P3–P4 22.80° for **6**. The intramolecular steric strain is, thus, unevenly distributed over the tetrapyrrole ligand backbone of these pentacoordinate species and mainly compensated for by the enhanced displacement of one of the terminal $\{C_4N\}$ rings.

The crystallographic determination of the fluorido complex **5** (Table 1) reveals a six-coordinate iron(III) ion.[38] The asymmetric unit contains a $[FeF_2(bdp)]^-$ ion, a Cs^+ counterion, and four disordered solvent molecules (dichloromethane and 2-propanol). Two such assemblies are connected by a center of inversion and form the unit cell. The iron(III) ion is bound by four nitrogen and two fluorine atoms in a distorted-octahedral geometry, with the fluorine donors occupying the axial positions at lengths of 1.926 and 1.912 Å (Figure 3). The nitrogen donors are asymmetrically bonded so that the inner Fe–N2 and Fe–N3 bonds are shorter than the outer bonds and that only two of the N-Fe-N angles are

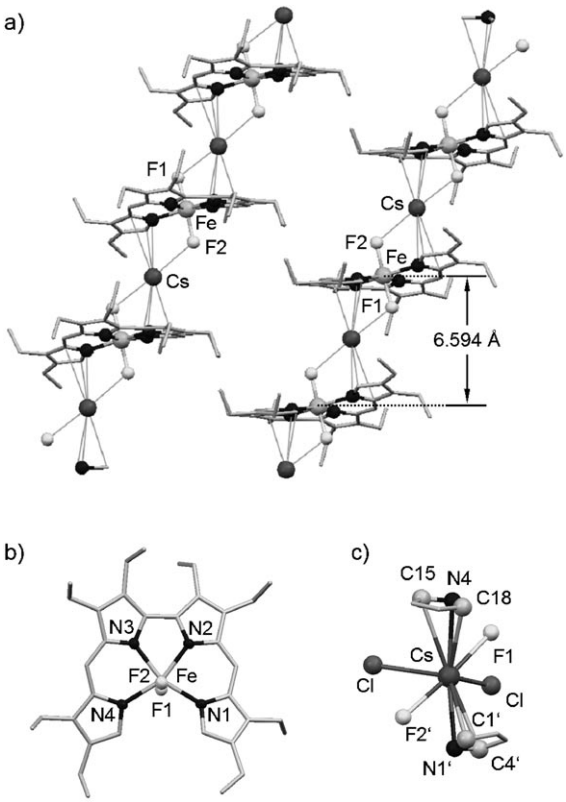

Figure 3. Results from the XRD study on $[Cs\{(bdp)FeF_2\}]$ (**5**·CsF). a) View in the crystallographic *b* direction: polymeric strands and distance between mean-square planes of the neighboring $\{FeN_4\}$ subunits (the hydrogen atoms and solvent molecules have been removed for clarity). b) Top view of the $[FeF_2(bdp)]^-$ complex ion. c) Coordination environment of the Cs^+ ion. Selected bond lengths [Å], distances [Å], and angles [°]: Fe–N1 2.106(4), Fe–N2 2.082(4), Fe–N3 2.080(4), Fe–N4 2.109(4), Fe–F1 1.926(3), Fe–F2 1.912(3), Cs–N1′ 3.395(4), Cs–N4 3.409(4), Cs–F1 2.947(3), Cs–F2 3.017(3); F1-Fe-F2 164.14(12), F1-Cs-F2 174.13(8), Fe-F1-Cs 115.40(12), Fe-F2-Cs 119.41(13).

found at about 90°. In addition, the F1-Fe-F2 angle of about 164° also clearly deviates from the ideal 180° of an octahedron. The Fe–N bonds of 2.080(4)-2.109(4) Å are significantly longer than those found for **2**, **6**, or **7** and point towards a high-spin configuration at the iron(III) ion in **5**·CsF. In addition, the helical distortion of the bidipyrrin backbone is more uniform than before and clearly decreased, as evident from the torsion angle N1-N2-N3-N4 of only 10.18°.

In the crystal of **5**·CsF, the ionic $[FeF_2(bdp)]^-$ complex units are connected to each other by cesium cations and form 1D polymeric chains in the *a* direction. The coordination sphere of the cesium ion is saturated by two fluorine donors, two chlorine atoms from cocrystallized dichloromethane, and two pyrrole rings of the complex ions, each of which is bonded in a (CNC)-η^3 mode. Two polymeric strands in antiparallel orientation extend through each unit cell, and two additional, disordered solvent molecules (dichloromethane and/or 2-propanol) stabilize the arrangement by the occupation of open clefts between the strands.

SQUID and Mössbauer investigations were carried out on microcrystalline samples of **2**, **6**, and **7** (Table 3). The coordi-

Table 3. Molecular magnetic moments and Mössbauer data for **2**, **6**, and **7**.

	2	**6**	**7**
$\mu_{eff}^{70\,K}$ [μ_B]	3.77	3.79	3.69
$\mu_{eff}^{350\,K}$ [μ_B]	4.32	4.02	3.89
$\delta_{Fe}^{298\,K}$	0.16 (0.24)[a]	0.15	0.14
$\Delta E_Q^{298\,K}$	3.08 (3.29)[a]	3.35	3.50

[a] Measured at 70 K.

nation polymer **5**·CsF was not introduced in this study because of the extreme hydrolytic sensitivity and unknown purity of the bulk compound. The pentacoordinate complexes **2**, **6**, and **7** are characterized by magnetic moments of 3.77, 3.79, and 3.69 μ_B, respectively, at 70 K, and the susceptibility measurements prove effective Curie–Weiss behavior up to about 150 K, as expected for isolated mononuclear transition-metal complexes. Above this temperature, however, the magnetic moments grow increasingly as shown for the most pronounced case [FeCl(bdp)] (**2**) in Figure 4. Mössbauer data for **2**, **6**, and **7** obtained at 298 K reveal one signal at 0.16, 0.15, and 0.14 mm s^{-1} with large quadrupole splitting values of 3.08, 3.35, and 3.50 mm s^{-1}, respectively, and a low-temperature determination carried out on the chlorido derivative **2** shows that the quadrupole splitting ΔE_Q reaches 3.29 mm s^{-1} at 70 K. The Mössbauer parameters, and in particular the large values for the quadrupole splitting ΔE_Q, strongly suggest that the iron(III) ions display a $S=3/2$ intermediate spin ground state in the solid state.[39–49] The same conclusion can be drawn from the effective magnetic moments of **2**, **6**, and **7** at 70 K, which are close to the spin-only value for a $S=3/2$ system of 3.88 μ_B.[50] The results fit nicely with the observed Fe–N bond lengths, which are clearly decreased with respect to high-spin iron(III) porphyrinoids.[35]

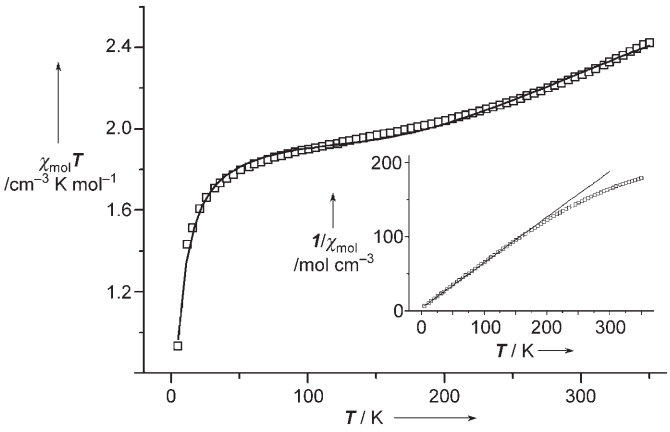

Figure 4. SQUID measurement of **2**: $\chi_{mol}T$ versus T with fit (spin-equilibrium model; fitting parameters: $\mu_{(3/2)}=3.88\,\mu_B$; $\theta_{(3/2)}=-4.5$ K; $\mu_{(5/2)}=5.92\,\mu_B$; $\theta_{(5/2)}=-1.0$ K; $T_a=760$ K; $\Delta H=-7.6$ kJ mol^{-1}), and plot of $1/\chi_{mol}$ versus T with Curie–Weiss fit (inset)).

Concerning the question of 3d electron configuration and bond lengths, an interesting comparison can be made with formally related chloridoiron–corroles[51–53] and the respective 2,2′-bidipyrrin **2**. For the latter, the equatorial Fe–N and Fe–Cl bonds are longer than in the macrocyclic counterparts, while the axial Fe–N bond lengths are rather similar for both systems. This observation points to the difference in the coordination polyhedron. In general, a depopulated $3d_{z^2}$ orbital should be expected for the open-chain compound **2**, while a depopulated $3d_{x^2-y^2}$ orbital is the rule for the macrocyclic iron chelates with square-pyramidal coordination. The assumed large amount of orbital mixing for the unsymmetric **2**, however, is expected to complicate this simple picture significantly.[54]

The increase in the magnetic moment with temperature has occasionally been observed in natural and artificial iron porphyrinoids and is usually explained by the Maltempo model, that is, by a spin admixed state of $S=3/2,5/2$ for this class of coordination compound.[55] In the cases described herein, however, the susceptibility data cannot be fitted with satisfying results using the Maltempo model, mainly as a result of the presence of an additional inflection point in the experimental $\chi_{mol}T$ versus T curve. A better description is derived from a simple $S=3/2/S=5/2$ spin-crossover scenario. Good fits were obtained using a simplified spin-equilibrium model without cooperativity and assuming spin-only cases with Curie–Weiss behavior for both the ground and excited states (Figure 4; for **6** and **7** see the Supporting Information).

Such a spin equilibrium is not necessarily in contrast with the observation of only one quadrupole doublet in the ambient temperature Mössbauer spectra. In principle, the phenomenon can be explained by taking into account a spin–flop relaxation that is fast on the timescale of the Mössbauer experiment. Similar cases have occasionally been discussed in the past for other spin-crossover processes,[56–59] and very recently a related case has been reported for an azidoiron–porphycene complex.[60] For a more detailed investigation into the spin dynamics of this class of bilinoid complex, however, additional measurements and derivatives will be necessary.

Behavior in solution: In the macrocyclic iron–porphyrinoid complexes, the electronic structure of the central metal atom is governed by the conformation of the tetrapyrrole and does not change significantly upon grinding or dissolving the crystals, although exceptions are known.[61] Open-chain tetrapyrrolic ligands on the other hand are much more flexible and may well be able to alter their conformation upon dissolution and with this the metal–ligand interaction and electronic structure. In addition, the conformational lock of the terminal hydrogen atoms of the bdp ligand could be overcome and allow the interconversion of the helices in solution, so that dynamic compounds result. Another aspect is the questionable stability of the hexacoordinate [FeF_2(bdp)]$^-$ ion, which can be expected to decompose in solution. Initial experiments were undertaken by X-band elec-

tron paramagnetic resonance (EPR) spectroscopy. The results for **2** and **5**·CsF are shown in Figure 5, and the data for all compounds are summarized in Table 4.

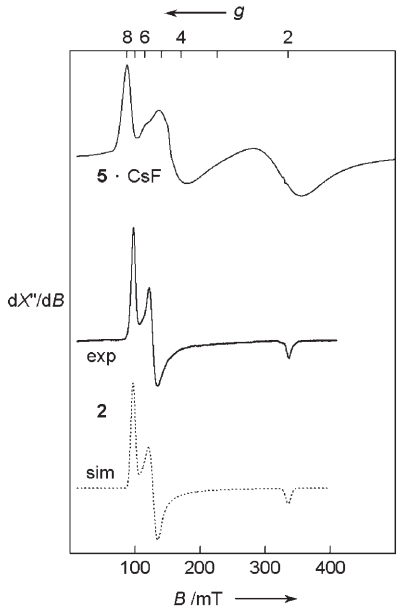

Figure 5. Top: X-band EPR spectra of **5**·CsF in frozen CH_2Cl_2 saturated with CsF at 30 K and **2** in frozen CH_2Cl_2 at 4 K (9.2250 GHz; 80 μW/34 dB, modulation frequency: 25.0 kHz, modulation amplitude: 1.00 mT). Center: experimental (exp) spectrum of **2**. Bottom: simulated (sim) spectrum (Easyspin-2.5.1[62]).

Table 4. Estimated (**5**·CsF) and simulated (**2**, **6**, and **7**) *g* values and rhombicity from EPR measurements.

	5·CsF	**2**	**6**	**7**
g_1	7.62	7.01	6.75	6.74
g_2	4.21	4.89	5.18	5.20
g_3	1.86	1.93	1.96	1.96
$E\,[D]$	–	$\leq$0.0097	$\leq$0.0090	$\leq$0.0094

The X-band EPR spectrum of [FeCl(bdp)] **2** measured in frozen dichloromethane at 4 K (Figure 5) shows a strongly rhombic and broadened signal with fitted values of $g_1 = 7.01$, $g_2 = 4.89$, and $g_3 = 1.93$. These values are expected for a non-axial iron(III) complex in the high-spin ($S = 5/2$) state without any visible $S = 3/2$ contamination.[63–67] Except for small differences in the *g* value and zero field splitting (zfs) rhombicity, the spectra of the bromido and iodido homologues **6** and **7** are identical and also show no sign of any intermediate spin admixture. The relatively broad absorptions of the compounds point to an unsymmetric, distorted geometry of the compounds in solution. An EPR spectrum of the fluorido complex **5** could be obtained in frozen dichloromethane saturated with CsF at 30 K (Figure 5, top trace). Even under these conditions, a mixture of different components is evident. The spectrum could not be fitted; however, the *g* values obtained directly from the measurements (Table 4) account for the presence of at least two high-spin iron(III) compounds, presumably the $[FeF_2(bdp)]^-$ ion and the pentacoordinate [FeF(bdp)] (**5**). As a result of the extremely high propensity of **5** to hydrolytic decay, however, additional contributions from the partially hydrolyzed material cannot be excluded in this case.

The transition from the C_2-symmetric hexacoordinate $[FeF_2(bdp)]^-$ ion to a pentacoordinate [FeF(bdp)] complex (**5**) with C_S symmetry can be monitored by using time-resolved ^{1}H NMR spectroscopic analysis in CD_2Cl_2 at ambient temperature. As shown in the upper trace in Figure 6, a

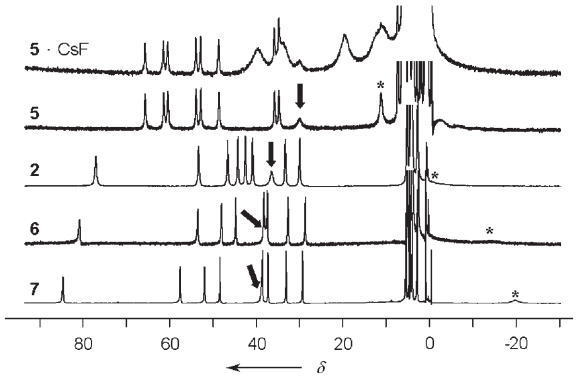

Figure 6. ^{1}H NMR spectra of the new iron chelates (400 MHz, CD_2Cl_2). Trace 1: spectrum of **5**·CsF directly after dissolution; trace 2: spectrum of **5**·CsF after 2 h in solution; trace 3: spectrum of [FeCl(bdp)] (**2**); trace 4: spectrum of [FeBr(bdp)] (**6**); trace 5: spectrum of [FeI(bdp)] (**7**). The resonance lines of the *meso* and α protons are marked by arrows and asterisks, respectively.

spectrum taken immediately after dissolution of **5**·CsF contains two distinct groups of signals in the region $\delta = 70$–10 ppm. Eight rather sharp signals appear low field between $\delta = 70$ and 35 ppm, which belong to the diastereotopic protons of four methylene groups in the pentacoordinate compound **5**. In addition, four broad signals are detected in the range $\delta = 45$–10 ppm, which disappear upon standing for two hours (second trace) and are, therefore, designated to the protons of four methylene groups of the C_2-symmetric $[FeF_2(bdp)]^-$ ion. The remaining broad signals at $\delta = 32$ and 21 ppm stem from the *meso*- and α-situated protons of **5**, respectively.

From a phenomenological point of view, the ^{1}H NMR spectra of **2**, **6**, and **7** (traces 3–5 in Figure 6) are very similar to the above-described spectrum of **5**, although the former display signals with smaller line-widths as no ligand-exchange process with excess halide anions can occur. The symmetry of the spectra indicates that the helix-inversion process is rapid on the timescale of the experiment. A variable-temperature (VT) NMR study undertaken on the chlorido derivative **2** shows neither a helix-inversion nor spin-transition process down to 190 K. The only visible effect is a continuous spread of the spectra with decreasing temperature, which unravels typical Curie behavior of the complex in solution between 290 and 190 K (see the Supporting Information). A very fast helix inversion is, however, more

probable than the assumption of a planar tetrapyrrole ligand in solution, since the high-spin compound **5**·CsF also maintains a pronounced helical conformation despite elongated Fe–N bonds.

The signal of the *meso*-situated hydrogen atom shifts to lower field with increasing size of the halide ligand. This behavior is a well-established feature of octaalkylporphyrins, albeit the signals are typically observed to be high field between $\delta = -40$ and -60 ppm for these compounds if a non-coordinating solvent is used.[68,69] The large deviation of the shifts indicates significant differences in the interactions of metal d electrons with the σ and π orbitals of the ligand, presumably originating from the helical conformation of the open-chain tetrapyrrole, and significant differences in the Fe···H distances. Notwithstanding this behavior, all the methylene and methyl group signals are observed in a range known for macrocyclic analogues throughout. A particularly strong influence of the axial ligand was observed for the shift of the signal for the terminal α-hydrogen atom. X-ray diffraction (XRD) studies prove that these hydrogen atoms are located only 3.113/3.255, 3.125/3.230, and 3.147/3.228 Å (for **2, 6**, and **7**, respectively) away from the paramagnetic iron center (as opposed to distances of about 4.5 Å for Fe···H_{meso}), so that an additional pseudocontact contribution might contribute to this peculiarity.[69] In contrast to the results in the solid state, the combined EPR and NMR spectroscopic studies thus suggest high-spin states for all species **2** and **5–7** in solution. The insufficient comparability of these new data with those of the intensely investigated macrocyclic iron–porphyrinoids does, however, leave a number of open questions that we are currently attempting to answer in our laboratories.

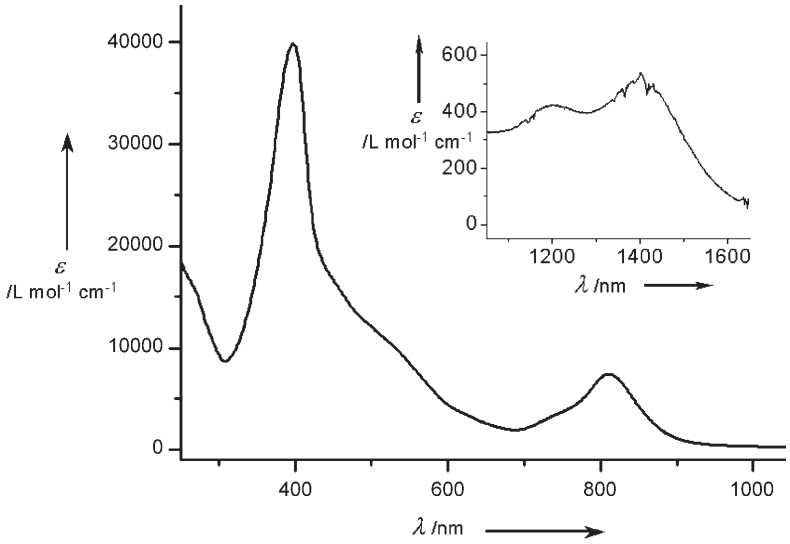

Figure 7. Electronic absorption spectra of **2** (CH_2Cl_2, 298 K). Large: UV/Vis spectrum; inset: NIR region.

The optical spectrum of **2** is unlike those spectra of the macrocyclic iron–porphyrinoids and displays the typical, broadened habitus in the UV/Vis region known for other bilins and bilin analogues (Figure 7).[70] As an interesting feature, additional bands were detected in the NIR region at 1200 and 1402 nm with molar extinctions of 420 and 540 $L\,mol^{-1}\,cm^{-1}$, respectively. Such low-energy bands are unknown for iron(III) porphyrins and indicate easily accessible ligand–metal charge transfer (LMCT) states in **2**.

Reactivity studies: From studies on related transition-metal complexes of bilin and bilindione ligands, it is well established that the central metal ion and the terminal α,ω positions of the tetrapyrrole compete for the most reactive sites in such molecules.[18,19,71] The reactivity of the terminal ligand positions has long and often been employed for metal-templated macrocyclization reactions in the synthesis of porphyrins,[72] corrins,[73–75] corroles,[76] and other porphyrinoids[77–79] from transition-metal bilinoids. In the case of the related verdoheme derivatives, several nucleophilic ring-opening reactions have been described to occur at this position with a range of nucleophiles.[80–84] For [FeCl(bdp)] (**2**), it can be expected that the iron ion is the most reactive site from a kinetic point of view, but that the thermodynamically stable products should result from the attack at the tetrapyrrole α,ω positions. Both reaction channels have been investigated with different nucleophiles (Scheme 3).

The action of a dilute solution of sodium hydroxide on **2** results in the expected formation of the dinuclear μ-oxido derivative **8**, which was isolated and characterized analytically (HRMS, elemental analysis) and spectroscopically (^{1}H NMR and Mössbauer spectroscopy) as a slightly paramagnetic compound with two antiferromagnetically coupled high-spin iron(III) ions. The treatment of a solution of **2** in dichloromethane with methanol, on the other hand, produces the demetalated species **9** and **10**, respectively, as the only isolated products. In addition to crystallographic determination of the molecular structure of **10** (Table 1; Figure 8, top), both new 2,2′-bidipyrrins were identified unambiguously by conventional techniques. The formation of both the mono- and disubstituted products **9** and **10** and the result of the control experiments, namely, free-base 2,2′-bidipyrrin does not undergo such a reaction in the presence of free iron(III) ions and methanol, point to a stepwise oxidative substitution process in the iron complex, followed by a strain-induced demetalation as proposed for FeBV-IXα.

Another question in this context arises from the expectation that methanol should replace the chlorido ligand from **2** and form a strongly solvated, hexacoordinate intermediate $[Fe(bdp)(MeOH)_2]^+$, as in **5**·CsF, prior to any ligand-substitution reaction. This intermediate, however, could not be

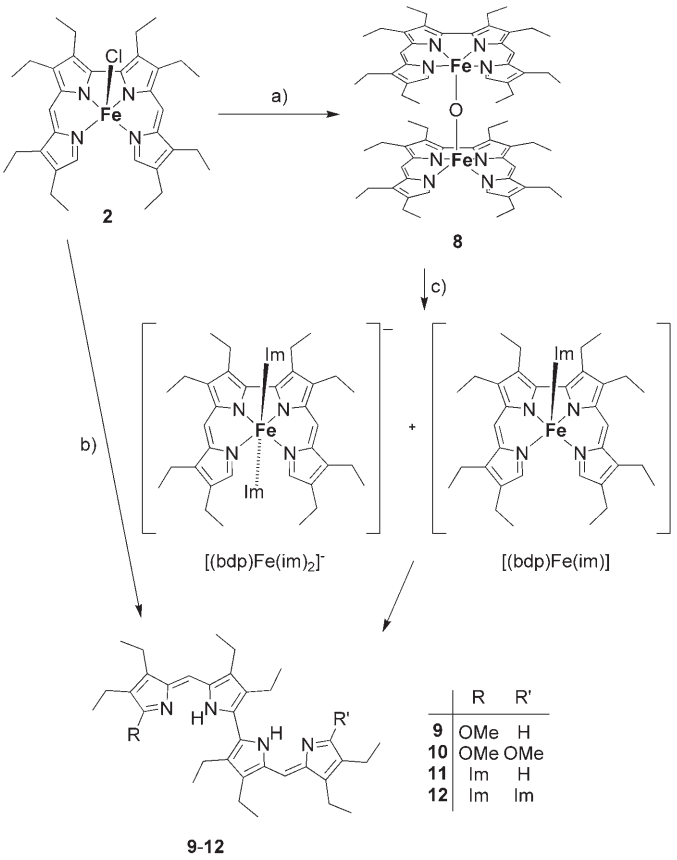

Scheme 3. Reactivity of [FeCl(bdp)] (**2**) with different nucleophiles. a) Dilute NaOH, CH_2Cl_2, air; b) MeOH, CH_2Cl_2, air; c) *N*-trimethylsilylimidazole, pentane, air.

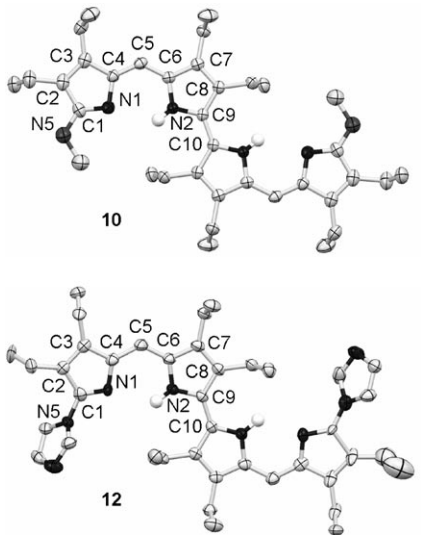

Figure 8. Selected views of the molecular structures of **10** and **12** (carbon-bound hydrogen atoms are removed for clarity; ellipsoids set at 50% probability).

isolated nor unambiguously observed by spectroscopic means. On the other hand, decomposition studies of **5**·CsF gave no hint of any fluorinated tetrapyrrole in the product mixture. Therefore, the action of stronger axial donors (phosphanes, N-heterocycles, thiolates, C-nucleophiles, and so forth) was investigated with **2**. In most cases, these experiments led to the fast and unselective decomposition of the starting material, which is reasonable when taking into account the general sensitivity of open-chain oligopyrroles against bases. This problem was overcome by the reaction of the μ-oxido dimer **8** with an excess of *N*-trimethylsilylimidazole in pentane, thus resulting in the selective precipitation of a ionic $[Fe(bdp)(im)_2]^-$ compound with an unknown counterion. In solution, this compound is extremely sensitive to dissociation and concomitant decay. The presence of a six-coordinate low-spin iron(III) ion, however, and the dissociation of one imidazolate ligand to form pentacoordinate [Fe(bdp)(im)] (Scheme 3) is strongly suggested by EPR and NMR spectroscopic data (see the Supporting Information). If the compound is dissolved in dichloromethane and stirred for 30 min, the complete decomposition and formation of two major products **11** and **12** is observed. This result is supported by spectroscopic analysis and crystallographic studies of **12** (Figure 8, bottom) and parallels the findings with the nucleophile MeOH.

Conclusion

In summary, we have achieved the preparation of a unique set of halogenidoiron(III) compounds with an open-chain tetrapyrrole ligand by decreasing the repulsive interactions between the termini of such bilinoids. These complexes are sufficiently stable for in-depth spectroscopic and structural characterization both in solution and the solid state. In solution, the iron(III) ions reside in a high-spin configuration as expected from related porphyrinoid compounds. The situation is different in the solid state, however, as the all available data from XRD, SQUID, and Mössbauer measurements correspond to the presence of an $S=3/2$ intermediate spin ground state, despite the unusual and strongly unsymmetric coordination of the iron(III) ion. In addition, the compounds display a spin dynamic in the solid state and CT transitions in solution, as shown by NIR spectroscopic analysis. Both findings differ from what is usually found for iron porphyrins. There is an intriguing possibility that such excited CT states play a supporting role for the observed reactivity of our novel complexes and that similar states may be key to explaining the extreme lability of FeBV-IXα outside the protein pocket. We will focus on this point and the exploitation of the high reactivity of these compounds in further investigations.

Experimental Section

The solvents were dried according to standard procedures and saturated with argon. All the reagents were purchased from commercial sources and used as received, if not stated otherwise. Diformyltetraethylbipyrrole

(**3**) and diethylpyrrole (**4**) were prepared following previously reported procedures.[85,86] The NMR spectra were obtained on a Bruker AMX 400 spectrometer. The chemical shifts (δ) are given in ppm relative to residual protio solvent resonances (^{1}H spectra). The mass spectra were recorded on a Finnigan 90 MAT (EI, FAB), Finnigan-MAT 95S (ESI), or Bruker Biflex IV (MALDI-TOF) instruments, and the *m/z* values are given for the most abundant isotopes only. The UV/Vis data were collected on a Shimadzu UV-1601 PC spectrophotometer. The NIR spectra were obtained using a Varian Cary 5000 instrument. SQUID measurements were performed on a Quantum Design MPMS R2 magnetometer. The X-band EPR spectra were recorded on a Bruker ESP-300 instrument. Mössbauer spectra were recorded on a conventional spectrometer equipped with a cryostat unit CF 500 (Oxford Instruments, UK). The isomer shift values are quoted relative to α-Fe.

Chlorido-(3,3′,4,4′,8,8′,9,9′-octaethyl-2,2′-bidipyrrinato)iron(III) (2): 3,4-Diethylpyrrole (**2**; 100 mg, 0.81 mmol) was treated under nitrogen with a solution of 3,3′,4,4′-tetraethyl-5,5′-diformyl-2,2′-bipyrrole (**1**; 100 mg, 0.33 mmol) in dichloromethane (15 mL) and $POCl_3$ (0.25 mL, 2.72 mmol), whereupon the reaction mixture changed from yellow to violet. The reaction mixture was stirred at ambient temperature for 20 min until blue-green. Triethylamine (2.0 mL) was added in air, and the resulting solution was immediately treated with a suspension of $FeCl_2{\cdot}4H_2O$ and $FeCl_3$ in dry dioxane (3 mL) and additional dioxane (80 mL) until the reaction mixture changed to brown. Dichloromethane (150 mL) and aqueous ammonia (2 mol L^{-1}, 50 mL) were then added quickly and the reaction mixture shaken until the organic layer became orange-brown. The organic layer was separated, dried with sodium sulfate, filtered, and the solvent removed in vacuo. The pure product was obtained from the residue by several quick recrystallization steps from dichloromethane/*n*-hexane and dichloromethane/2-propanol, in which the compound was dissolved first and then the dichloromethane was removed at 400 mbar. After washing with *n*-hexane and drying in high vacuo, the title compound was obtained as a violet-black, microcrystalline solid (84 mg, 42 %). ^{1}H NMR (CD_2Cl_2, 20 °C): δ = 77.18 (brs, 2H), 54.23 (brs, 2H), 47.13 (brs, 2H), 44.74 (brs, 2H), 43.65 (brs, 2H), 41.73 (brs, 2H), 36.92 (brs, 2H), 33.97 (brs, 2H), 30.79 (brs, 2H), 5.84 (brs, 6H), 4.94 (brs, 6H), 4.64 (brs, 6H), 3.43 ppm (brs, 6H); the broad signal for the α protons was obscured by the methyl group signals; UV/Vis/NIR (CH_2Cl_2): λ_{max} (ε) = 388 (39800), 812 (7430), 1202 (450), 1404 nm (530 mol^{-1} m^3 cm^{-1}); HRMS (MALDI-TOF): *m/z* 599.2605 calcd for $[M]^+$: 599.2604; elemental analysis calcd (%) for $C_{34}H_{44}N_4ClFe$ (600.04): C 68.06, H 7.39, N 9.34; found: C 67.85, H 7.27, N 8.96.

Fluorido-(3,3′,4,4′,8,8′,9,9′-octaethyl-2,2′-bidipyrrinato)iron(III) (5)·CsF: Prepared from chlorido complex **3** (100 mg, 0.17 mmol) in dry dichloromethane (4 mL) by treatment with cesium fluoride in dry 2-propanol (3 mL), layering with pentane and crystallization at −30 °C as dark purple crystals (19.0 mg, 19 %). ^{1}H NMR (CD_2Cl_2, 25 °C): signals for the CsF adduct at δ = 40.66 (brs, 4H), 34.98 (br s, 4H), 20.37 (brs, 4H), 12.24 (brs, 4H), 2.59 ppm (brs, 24H); signals for the pentacoordinate complex at δ = 66.99 (brs, 2H), 62.66 (brs, 2H), 61.71 (brs, 2H), 55.12 (brs, 2H), 53.99 (br s, 2H), 49.72 (brs, 2H), 36.79 (brs, 2H), 35.66 (brs, 2H), 30.83 (brs, 2H), 6.88 (brs, 6H), 6.45 (brs, 6H), 5.49 (brs, 6H), 4.50 ppm (brs, 6H); the broad signals for the other α and *meso* protons are hidden; HRMS (ESI): *m/z* 602.2878 calcd for $[M+F]^-$: 602.2863.

Bromido-(3,3′,4,4′,8,8′,9,9′-octaethyl-2,2′-bidipyrrinato)iron(III) (6): A mixture of chlorido complex **3** (100 mg, 0.17 mmol) and LiBr (1.10 g, 12.7 mmol) was treated with dichloromethane (5 mL) and 2-propanol (15 mL) and heated under inert conditions until all the solids were dissolved. The red-brown solution was stirred over night at ambient temperature and reduced in vacuo to a fifth of the volume, whereupon the product crystallized as a dark solid. The solid was filtered, washed several times with 2-propanol, and then dissolved in dichloromethane. To remove traces of LiBr, this solution was washed with water (2 × 50 mL), dried with sodium sulfate, treated with *n*-hexane (10 mL), and evaporated to dryness on a rotatory evaporator. Washing the residue with hexane and drying in high vacuo yielded **5** in analytic purity (101 mg, 94 %). ^{1}H NMR (CD_2Cl_2, 20 °C): δ = 82.35 (brs, 2H), 54.71 (brs, 2H), 49.15 (brs, 2H), 45.82 (brs, 2H), 39.27 (brs, 2H), 38.87 (brs, 2H), 38.46 (brs, 2H), 33.64 (brs, 2H), 29.31 (brs, 2H), 5.80 (brs, 6H), 4.72 (brs, 6H), 4.47 (brs, 6H), 3.24 (brs, 6H), −14.04 ppm (brs, 2H); UV/Vis (CH_2Cl_2): λ_{max} = 386, 806 nm; HRMS (MALDI-TOF): *m/z* 643.2099 calcd for $[M]^+$: 643.2137; elemental analysis calcd (%) for $C_{34}H_{44}N_4BrFe$ (644.49): C 63.36, H 6.88, N 8.69; found: C 63.31, H 7.01, N 8.43.

Iodido-(3,3′,4,4′,8,8′,9,9′-octaethyl-2,2′-bidipyrrinato)iron(III) (7): A mixture of chlorido complex **3** (100 mg, 0.17 mmol) and NaI (1.10 g, 7.3 mmol) was treated with acetone (15 mL) and heated under inert conditions until all the solids dissolved. The red-brown solution was stirred for 3 h at ambient temperature, filtered, and reduced in vacuo to dryness. The solid was redissolved in dichloromethane, filtered, and washed with water (2 × 50 mL). After drying with sodium sulfate, this solution was treated with *n*-hexane (10 mL) and evaporated to dryness on the rotatory evaporator. Washing the residue with hexane and drying in high vacuo yielded **6** in analytic purity (94 mg, 80 %). ^{1}H NMR (CD_2Cl_2, 20 °C): δ = 87.88 (brs, 2H), 59.59 (brs, 2H), 54.48 (brs, 2H), 50.82 (brs, 2H), 40.39 (brs, 2H), 40.09 (brs, 2H), 38.68 (brs, 2H), 34.63 (brs, 2H), 30.76 (brs, 2H), 6.28 (brs, 6H), 5.13 (brs, 6H), 4.67 (br s, 6H), 3.55 (brs, 6H), −20.09 ppm (brs, 2H); UV/Vis (CH_2Cl_2): λ_{max} = 387, 816 nm; HRMS (MALDI-TOF): *m/z* 564.2923 calcd for $[M-I]^+$: 564.2915; elemental analysis calcd (%) for $C_{34}H_{44}N_4IFe$ (691.49): C 59.06, H 6.41, N 8.10; found: C 58.69, H 6.33, N 7.79.

μ-Oxido[bis(3,3′,4,4′,8,8′,9,9′-octaethyl-2,2′-bidipyrrinato)iron(III)] (8): A solution of [FeCl(bdp)] (**2**; 100 mg, 0.17 mmol) in dichloromethane (100 mL) was shaken with a solution of NaOH (1 mol L^{-1}, 100 mL). The organic layer was dried with sodium sulfate and the solvent removed to leave **8** as a microcrystalline solid (96 mg, 99 %). ^{1}H NMR (CD_2Cl_2, 20 °C): δ = 11.90 (brs, 4H), 8.05 (brs, 4H), 7.98/6.03 (br AB, 8H), 7.14/6.14 (br AB, 8H), 5.17/4.66 (br AB, 8H), 5.09/4.28 (br AB, 8H), 1.49 (brs, 12H), 1.35 (brs, 24H), 1.28 ppm (brs, 12H); UV/Vis (CH_2Cl_2): λ_{max} = 375 sh, 399, 446 sh, 733, 798 nm; Mössbauer: (α-Fe, RT): δ_{iso} = 0.26 mm s^{-1}, ΔE_Q = 0.83 mm s^{-1}; HRMS (ESI): *m/z* 1145.5873 calcd for $[M+H]^+$: 1145.5853; elemental analysis calcd (%) for $C_{68}H_{88}N_8Fe_2O$ (1145.17): C 71.32, H 7.75, N 9.78; found: C 70.96, H 7.73, N 9.44.

3,3′,4,4′,8,8′,9,9′-Octaethyl-10-methoxy-2,2′-bidipyrrin (9) and 3,3′,4,4′,8,8′,9,9′-octaethyl-10,10′-methoxy-2,2′-bidipyrrin (10): A solution of **2** (100 mg, 0.17 mmol) in methanol (100 mL) was stirred in air for 1 week. The solvent was evaporated and the residue subjected to chromatography on alumina (activity II) with *n*-hexane/dichloromethane as the eluant (1:1) to obtain **10** as the major pink band with strong red fluorescence (38.8 mg, 40 %) and **9** as a smaller purple band with weak red fluorescence (3.8 mg, 4 %).

9: ^{1}H NMR (C_6D_6, 20 °C): δ = 11.91 (brs, 1H, NH), 6.99 (s, 1H, *meso*-H), 6.87 (s, 1H, *meso*-H), 6.72 (s, 1H, term-H), 3.84 (s, 3H, OCH_3), 3.26 (q, 2H, J = 7.4 Hz, CH_2), 2.86 (q, 2H, J = 7.5 Hz, CH_2), 2.68 (q, 2H, J = 7.6 Hz, CH_2), 2.63 (q, 2H, J = 7.6 Hz, CH_2), 2.53 (q, 2H, J = 7.6 Hz, CH_2), 2.48 (q, 2H, J = 7.5 Hz, CH_2), 2.40 (q, 2H, J = 7.6 Hz, CH_2), 2.38 (q, 2H, J = 7.5 Hz, CH_2), 1.62 (t, 3H, J = 7.4 Hz, CH_3), 1.26 (t, 3H, J = 7.5 Hz, CH_3), 1.24 (t, 3H, J = 7.6 Hz, CH_3), 1.22 (t, 3H, J = 7.6 Hz, CH_3), 1.21 (t, 3H, J = 7.5 Hz, CH_3), 1.19 (t, 3H, J = 7.6 Hz, CH_3), 1.16 (t, 3H, J = 7.5 Hz, CH_3), 1.12 ppm (t, 3H, J = 7.6 Hz, CH_3); ^{13}C NMR (C_6D_6, 20 °C): δ = 175.0, 156.6, 147.6, 147.5, 146.0, 144.9, 135.0, 134.1, 132.5, 131.3, 130.2, 130.0, 129.9, 128.9, 127.5, 126.2, 115.6, 110.5, 55.3, 19.7, 19.6, 18.6, 18.1, 17.7, 17.4 (2C), 17.5, 17.3, 17.1, 16.7 (2C), 16.0, 15,6, 15.2, 14.5 ppm; HRMS (MALDI-TOF): *m/z* 540.3834 calcd for $[M]^+$: 540.3828.

10: ^{1}H NMR (C_6D_6, 20 °C): δ = 11.85 (brs, 2H, NH), 6.75 (s, 2H, *meso*-H), 3.80 (s, 6H, OCH_3), 2.90 (q, 4H, J = 7.5 Hz, CH_2), 2.67 (q, 4H, J = 7.6 Hz, CH_2), 2.42 (q, 4H, J = 7.6 Hz, CH_2), 2.38 (q, 4H, J = 7.5 Hz, CH_2), 1.30 (t, 6H, J = 7.5 Hz, CH_3), 1.26 (t, 6H, J = 7.6 Hz, CH_3), 1.18 (t, 6H, J = 7.5 Hz, CH_3), 1.12 ppm (t, 6H, J = 7.6 Hz, CH_3); ^{13}C NMR (C_6D_6, 20 °C): δ = 174.3, 147.3, 143.8, 131.8, 128.6, 127.3, 126.9, 124.6, 110.7, 55.2, 18.6, 18.1, 18.0, 17.5, 17.4, 16.8, 16.5, 14.5 ppm; HRMS (ESI): *m/z* 570.3928 calcd for $[M]^+$: 540.3930.

Reaction of [{Fe(bdp)}$_2$O] (8) with trimethylsilylimidazole and decomposition to 11 and 12: The μ-oxido derivative **8** (18 mg, 0.016 mmol) was dissolved in pentane (10 mL) and treated with trimethylsilylimidazole (10 μL) for 10 min. A fine, dark precipitate containing the ionic $[Fe(bdp)(im)_2]^-$ complex formed and was filtered, carefully washed with sev-

eral aliquots of dry pentane, and dried in high vacuo to yield 20 mg of the crude product. MS (ESI): *m/z* 701 $[M+H]^+$, 632 $[M-im+H]^+$, 564 $[M-2im]^+$.

The dark solid from the above preparation was dissolved in dichloromethane (10 mL) and stirred at ambient temperature for 30 min. During this time, a color change from brown to brown-green, green, and finally petrol blue was observed. Purification by column chromatography of the resulting mixture on alumina III with *n*-hexane/dichloromethane (4:1) yields **11** and **12** in a blue and turquoise band, respectively, as the only nonpolymeric products in 18 and 35% yield, respectively.

11: ^{1}H NMR (CD_2Cl_2, 20°C): δ = 11.79 (brs, 2H, NH), 8.06, 7.51, 7.17 (s, 3H, Im-H), 7.02 (s, 1H, term-H), 6.93, 6.84 (s, 2H, *meso*-H), 2.97 (q, J = 7.4 Hz, 2H, CH_2), 2.82 (q, J = 7.4 Hz, 2H, CH_2), 2.74 (q, J = 7.5 Hz, 2H, CH_2), 2.71–2.60 (m, 6H, CH_2), 2.57 (q, J = 7.5 Hz, 2H, CH_2), 2.49 (q, J = 7.5 Hz, 2H, CH_2), 1.35 (t, J = 7.4 Hz, 3H, CH_3), 1.28–1.17 (m, 15H, CH_3), 1.09 (t, J = 7.4 Hz, 3H, CH_3), 1.02 ppm (t, J = 7.6 Hz, 3H, CH_3); ^{13}C NMR (CD_2Cl_2, 20°C): δ = 157.5, 154.3, 149.6, 146.3, 146.2, 143.9, 137.6, 135.8, 134.4, 133.6, 131.3, 130.5, 129.5, 128.8, 128.2, 136.2, 129.7, 118.0, 128.3, 117.7, 116.9, 19.2, 19.0, 18.2, 18.1, 17.8, 17.7, 17.4, 17.2, 17.0, 16.9, 16.7, 15.2, 15.1, 14.7, 14.6 ppm; HRMS (ESI): *m/z* 577.4010 calcd for $[M+1]^+$: 577.4013.

12: ^{1}H NMR (CD_2Cl_2, 20°C): δ = 11.69 (brs, 2H, NH), 8.04, 7.58, 7.14 (s, 3H, Im-H), 6.91, (s, 2H, *meso*-H), 2.81 (q, J = 7.2 Hz, 4H, CH_2), 2.70 (q, J = 7.4 Hz, 4H, CH_2), 2.67 (q, J = 7.4 Hz, 4H, CH_2), 2.56 (q, J = 7.4 Hz, 4H, CH_2), 1.24 (t, J = 7.5 Hz, 6H, CH_3), 1.23 (t, J = 7.6 Hz, 6H, CH_3), 1.09 (t, J = 7.5 Hz, 6H, CH_3) 1.07 ppm (t, J = 7.5 Hz, 6H, CH_3); ^{13}C NMR (CD_2Cl_2, 20°C): δ = 157.2, 149.6, 143.7, 138.1, 136.4, 130.3, 130.0, 129.7, 128.7, 127.1, 118.2, 117.7, 18.6, 18.4, 18.1, 17.8, 17.4, 17.2, 15.7, 14.9 ppm; HRMS (ESI): *m/z* 643.4235 calcd for $[M+Na]^+$: 643.4231.

X-ray crystallographic study of 2, 5–7, 10, and 12: Suitable crystals of the complexes **2**, **6**, **7**, **10**, and **12** were obtained by layering concentrated solutions of the compounds in dichloromethane with *n*-hexane and allowing slow diffusion below room temperature. A crystal of **5**·CsF grew as the solvate from the reaction mixture at −40°C. Data was recorded on a Stoe IPDS-1 instrument. The crystallographic data and experimental details are given in Table 1. CCDC-669457, CCDC-669458, CCDC-669459, CCDC-669460, CCDC-669461, CCDC-669462 contain the supplementary crystallographic data for this paper. These data can be obtained free of charge from The Cambridge Crystallographic Data Centre via www.ccdc.cam.ac.uk/data_request/cif.

Acknowledgements

Financial support by the Deutsche Forschungsgemeinschaft (DFG) is gratefully acknowledged. We thank Dr. Christian Kleeberg for assistance with the crystal structure of **5**·CsF and Robin Krüger for technical support.

[1] P. R. Ortiz de Montellano, A. Wilks, *Adv. Inorg. Chem.* **2001**, *51*, 359–407.
[2] P. R. Ortiz de Montellano, *Curr. Opin. Chem. Biol.* **2000**, *4*, 221–227.
[3] Y. Liu, P. R. Ortiz de Montellano, *J. Biol. Chem.* **2000**, *275*, 5297–5307.
[4] M. Sugishima, H. Sakamoto, Y. Higashimoto, M. Noguchi, K. Fukuyama, *J. Biol. Chem.* **2003**, *278*, 32352–32358.
[5] L. Lad, J. Friedman, H. Y. Li, B. Bhaskar, P. R. Ortiz de Montellano, T. L. Poulos, *Biochemistry* **2004**, *43*, 3793–3801.
[6] J.-H. Fuhrhop, P. K. W. Wasser, J. Subramanian, U. Schrader, *Liebigs Ann. Chem.* **1974**, 1450–1466.
[7] J.-H. Fuhrhop, A. Salek, J. Subramanian, C. Mengersen, S. Besecke, *Liebigs Ann. Chem.* **1975**, 1131–1147.
[8] A. L. Balch, L. Latos-Grażyński, B. C. Noll, M. M. Olmstead, N. Safari, *J. Am. Chem. Soc.* **1993**, *115*, 9056–9061.
[9] R. Koerner, L. Latos- Grażyński, A. L. Balch, *J. Am. Chem. Soc.* **1998**, *120*, 9246–9255.
[10] K. T. Nguyen, S. P. Rath, L. Latos- Grażyński, M. M. Olmstead, A. L. Balch, *J. Am. Chem. Soc.* **2004**, *126*, 6210–6211.
[11] J. Subramanian, J. H. Fuhrhop, in *The Porphyrins* (Ed.: D. Dolphin), Academic Press, New York **1978**, *Vol. 2*, pp. 255–285.
[12] W. S. Sheldrick, J. Engel, *J. Chem. Soc. Chem. Commun.* **1980**, 5–6.
[13] R. Bonnett, D. G. Buckley, D. Hamzetash, *J. Chem. Soc. Perkin Trans. 1* **1981**, 322–325.
[14] A. L. Balch, M. Mazzanti, B. C. Noll, M. M. Olmstead, *J. Am. Chem. Soc.* **1994**, *116*, 9114–9122.
[15] R. G. Khoury, M. O. Senge, J. E. Colchester, K. M. Smith, *J. Chem. Soc. Dalton Trans.* **1996**, 3937–3950.
[16] T. Mizutani, S. Yagi, A. Honmaru, H. Ogoshi, *J. Am. Chem. Soc.* **1996**, *118*, 5318–5319.
[17] Y. Zhang, A. Thompson, S. J. Rettig, D. Dolphin, *J. Am. Chem. Soc.* **1998**, *120*, 13537–13538.
[18] R. Koerner, M. M. Olmstead, A. Ozarowski, S. L. Phillips, P. M. Van Calcar, K. Winkler, A. L. Balch, *J. Am. Chem. Soc.* **1998**, *120*, 1274–1284.
[19] P. A. Lord, B. C. Noll, M. M. Olmstead, A. L. Balch, *J. Am. Chem. Soc.* **2001**, *123*, 10554–10559.
[20] M. Bröring, C. D. Brandt, J. Lex, H.-U. Humpf, J. Bley-Escrich, J.-P. Gisselbrecht, *Eur. J. Inorg. Chem.* **2001**, 2549–2556.
[21] I. Spasojević, I. Batiní-Haberle, R. D. Stevens, P. Hambright, A. N. Thorpe, J. Grodkowski, P. Neta, I. Fridovich, *Inorg. Chem.* **2001**, *40*, 726–739.
[22] M. Bröring, C. D. Brandt, J. Bley-Escrich, J.-P. Gisselbrecht, *Eur. J. Inorg. Chem.* **2002**, 910–917.
[23] T. E. Wood, N. D. Dalgleish, E. D. Power, A. Thompson, X. Chen, Y. Okamoto, *J. Org. Chem.* **2005**, *70*, 9967–9978.
[24] H. S. Gill, I. Finger, I. Bozidarevic, F. Szydlo, M. J. Scott, *New J. Chem.* **2005**, *29*, 68–72.
[25] M. Bröring, S. Link, C. D. Brandt, E. Cónsul Tejero, *Eur. J. Inorg. Chem.* **2007**, 1661–1670.
[26] M. Bröring, *Synthesis* **2000**, 1291–1294.
[27] M. Bröring, D. Griebel, C. Hell, A. Pfister, *J. Porphyrins Phthalocyanines* **2001**, *5*, 708–714.
[28] M. Bröring, C. D. Brandt, *Monatsh. Chem.* **2002**, *133*, 623–630.
[29] M. Bröring, C. D. Brandt, E. Cónsul Tejero, *Z. Anorg. Allg. Chem.* **2005**, *631*, 1793–1798.
[30] M. Bröring, E. Cónsul-Tejero, *J. Organomet. Chem.* **2005**, *690*, 5290–5299.
[31] M. Bröring, C. Hell, *Chem. Commun.* **2001**, 2336–2337.
[32] M. Bröring, C. Hell, C. D. Brandt, E. Cónsul Tejero, *J. Porphyrins Phthalocyanines* **2003**, *7*, 214–219.
[33] M. Bröring, F. Brégier, E. Cónsul Tejero, C. Hell, M. C. Holthausen, *Angew. Chem.* **2007**, *119*, 449–452; *Angew. Chem. Int. Ed.* **2007**, *46*, 445–448.
[34] M. Bröring, C. Hell, F. Brégier, O. Burghaus, E. Cónsul Tejero, *Inorg. Chem.* **2007**, *46*, 5477–5479.
[35] W. R. Scheidt, in *The Porphyrin Handbook* (Eds: K. M. Kadish, K. M. Smith, R. Guilard), Academic Press, San Diego **2000**, *Vol. 3*, pp. 49–112.
[36] Y. Ohgo, S. Neya, T. Ikeue, M. Takahashi, M. Takeda, N. Funasaki, M. Nakamura, *Inorg. Chem.* **2002**, *41*, 4627–4629.
[37] J. P. Fitzgerald, B. S. Haggerty, A. L. Rheingold, L. May, G. A. Brewer, *Inorg. Chem.* **1992**, *31*, 2006–2013.
[38] A similar case has been reported for the $[FeF_2(tpp)]^-$ ion: W. R. Scheidt, Y. J. Lee, S. Tamai, K. Hatano, *J. Am. Chem. Soc.* **1983**, *105*, 778–782.
[39] H. H. Wickman, C. F. Wagner, *J. Chem. Phys.* **1969**, *51*, 435–444.
[40] K. L. Kostka, B. G. Fox, M. P. Hendrich, T. J. Collins, C. E. F. Rickard, L. J. Wright, E. Münck, *J. Am. Chem. Soc.* **1993**, *115*, 6746–6757.
[41] J. P. Fitzgerald, G. P. A. Yap, A. L. Rheingold, C. T. Brewer, L. May, G. A. Brewer, *J. Chem. Soc. Dalton Trans.* **1996**, 1249–1253.
[42] W. O. Koch, V. Schünemann, M. Gerdan, A. X. Trautwein, H.-J. Krüger, *Chem. Eur. J.* **1998**, *4*, 686–691.

[43] M. Fettouhi, M. Morsy, A. Waheed, S. Golhen, L. Ouahab, J. P. Sutter, O. Kahn, N. Menendez, F. Varret, *Inorg. Chem.* **1999**, *38*, 4910–4912.
[44] D. R. Evans, C. A. Reed, *J. Am. Chem. Soc.* **2000**, *122*, 4660–4667.
[45] J. P. Simonato, J. Pecaut, L. Le Pape, J. L. Oddou, C. Jeandey, M. Shang, W. R. Scheidt, J. Wojaczyński, S. Wołowiec, L. Latos-Grażyński, J. C. Marchon, *Inorg. Chem.* **2000**, *39*, 3978–3987.
[46] T. Ikeue, Y. Ohgo, T. Yamaguchi, M. Takahashi, M. Takeda, M. Nakamura, *Angew. Chem.* **2001**, *113*, 2687–2690; *Angew. Chem. Int. Ed.* **2001**, *40*, 2617–2620.
[47] O. Zakharieva, V. Schünemann, M. Gerdan, S. Licoccia, S. Cai, F. A. Walker, A. X. Trautwein, *J. Am. Chem. Soc.* **2002**, *124*, 6636–6648.
[48] P. Ghosh, E. Bill, T. Weyhermüller, K. Wieghardt, *J. Am. Chem. Soc.* **2003**, *125*, 3967–3979.
[49] K. Ray, E. Bill, T. Weyhermüller, K. Wieghardt, *J. Am. Chem. Soc.* **2005**, *127*, 5641–5654.
[50] O. Kahn, *Molecular Magnetism*, VCH, Weinheim **1993**.
[51] E. Vogel, S. Will, A. Schulze-Tilling, L. Neumann, J. Lex, E. Bill, A. X. Trautwein, K. Wieghardt, *Angew. Chem.* **1994**, *106*, 771–775; *Angew. Chem. Int. Ed. Engl.* **1994**, *33*, 731–735.
[52] L. Simkhovich, N. Galili, I. Saltsman, I. Goldberg, Z. Gross, *Inorg. Chem.* **2000**, *39*, 2704–2705.
[53] S. Nardis, R. Paolesse, S. Licoccia, F. R. Fronczek, M. G. H. Vicente, T. K. Shokhireva, S. Cai, F. A. Walker, *Inorg. Chem.* **2005**, *44*, 7030–7046.
[54] I. Wasbotten, A. Ghosh, *Inorg. Chem.* **2006**, *45*, 4914–4921.
[55] M. M. Maltempo, *J. Chem. Phys.* **1974**, *61*, 2540–2547.
[56] P. B. Merrithew, P. G. Rasmussen, *Inorg. Chem.* **1972**, *11*, 325–330.
[57] M. S. Haddad, W. D. Federer, M. W. Lynch, D. N. Hendrickson, *J. Am. Chem. Soc.* **1980**, *102*, 1468–1470.
[58] M. S. Haddad, M. W. Lynch, W. D. Federer, D. N. Hendrickson, *Inorg. Chem.* **1981**, *20*, 123–131.
[59] M. S. Haddad, W. D. Federer, M. W. Lynch, D. N. Hendrickson, *Inorg. Chem.* **1981**, *20*, 131–139.
[60] S. Neya, A. Takahashi, H. Ode, T. Hoshino, M. Hata, A. Ikezaki, Y. Ohgo, M. Takahashi, H. Hiramatsu, T. Kitagawa, Y. Furutani, H. Kandori, N. Funasaki, M. Nakamura, *Eur. J. Inorg. Chem.* **2007**, 3188–3194.
[61] A. Tabard, P. Cocolios, G. Lagrange, R. Gerardin, J. Hubsch, C. Lecomte, J. Zarembowitch, R. Guilard, *Inorg. Chem.* **1988**, *27*, 110–117.
[62] S. Stoll, A. Schweiger, *J. Magn. Reson.* **2006**, *178*, 42–55.
[63] M. E. Kastner, W. R. Scheidt, T. Mashiko, C. A. Reed, *J. Am. Chem. Soc.* **1978**, *100*, 666–667.
[64] C. A. Reed, T. Mashiko, S. P. Bentley, M. E. Kastner, W. R. Scheidt, K. Spartalian, G. Lang, *J. Am. Chem. Soc.* **1979**, *101*, 2948–2958.
[65] M. M. Maltempo, T. H. Moss, K. Spartalian, *J. Chem. Phys.* **1980**, *73*, 2100–2106.
[66] R. J. Cheng, P. Y. Chen, P. R. Gau, P. R. C. C. Chen, S. M. Peng, *J. Am. Chem. Soc.* **1997**, *119*, 2563–2569.
[67] V. Schünemann, M. Gerdan, A. X. Trautwein, N. Haoudi, D. Mandon, J. Fischer, R. Weiss, A. Tabard, R. Guilard, *Angew. Chem.* **1999**, *111*, 3376–3379; *Angew. Chem. Int. Ed.* **1999**, *38*, 3181–3183.
[68] F. A. Walker, in *The Porphyrin Handbook* (Eds: K. M. Kadish, K. M. Smith, R. Guilard), Academic Press, San Diego **2000**, *Vol. 5*, pp. 121–129.
[69] G. N. La Mar, F. A. Walker, in *The Porphyrins* (Ed.: D. Dolphin), Academic Press, New York **1979**, *Vol. IVB*, pp. 57–161.
[70] H. Falk, *The Chemistry of Linear Oligopyrroles and Bile Pigments*, Springer, Vienna, **1989**.
[71] S. Attar, A. Ozarowski, P. M. Van Calcar, K. Winkler, A. L. Balch, *Chem. Commun.* **1997**, 1115–1116.
[72] K. M. Smith, in *The Porphyrin Handbook* (Eds: K. M. Kadish, K. M. Smith, R. Guilard), Academic Press, San Diego **2000**, *Vol. 1*, pp. 119–148.
[73] R. L. N. Harris, A. W. Johnson, I. T. Kay, *J. Chem. Soc. Chem. Commun.* **1965**, 355–356.
[74] D. Dolphin, R. L. N. Harris, J. L. Huppatz, A. W. Johnson, I. T. Kay, *J. Chem. Soc. C* **1966**, 30–39.
[75] D. A. Clarke, R. Grigg, R. L. N. Harris, A. W. Johnson, I. T. Kay, K. W. Shelton, *J. Chem. Soc. C* **1967**, 1648–1656.
[76] Y. Murakami, Y. Matsuda, K. Sakata, S. Yamada, Y. Tanaka, Y. Aoyama, *Bull. Chem. Soc. Jpn.* **1981**, *54*, 163–169.
[77] H. Xie, K. M. Smith, *Tetrahedron Lett.* **1992**, *33*, 1197–1200.
[78] E. Vogel, B. Binsack, Y. Hellwig, C. Erben, A. Heger, J. Lex, Y.-D. Wu, *Angew. Chem.* **1997**, *109*, 2725–2728; *Angew. Chem. Int. Ed. Engl.* **1997**, *36*, 2612–2615.
[79] E. Vogel, M. Bröring, C. Erben, R. Demuth, J. Lex, M. Nendel, K. N. Houk, *Angew. Chem.* **1997**, *109*, 363–367; *Angew. Chem. Int. Ed. Engl.* **1997**, *36*, 353–357.
[80] J.-H. Fuhrhop, P. Krüger, *Liebigs Ann. Chem.* **1977**, 360–370.
[81] L. Latos-Grażyński, J. Johnson, S. Attar, M. M. Olmstead, A. L. Balch, *Inorg. Chem.* **1998**, *37*, 4493–4499.
[82] J. A. Johnson, M. M. Olmstead, A. L. Balch, *Inorg. Chem.* **1999**, *38*, 5379–5383.
[83] J. A. Johnson, M. M. Olmstead, A. M. Stolzenberg, A. L. Balch, *Inorg. Chem.* **2001**, *40*, 5585–5595.
[84] L. Latos- Grażyński, J. Wojaczyński, R. Koerner, J. J. Johnson, A. L. Balch, *Inorg. Chem.* **2001**, *40*, 4971–4977.
[85] M. J. Broadhurst, R. Grigg, A. W. Johnson, *J. Chem. Soc. Perkin Trans. 1* **1972**, 2111–2116.
[86] J. L. Sessler, A. Mozaffari, M. R. Johnson, *Org. Synth.* **1992**, *70*, 68–78.
[87] G. M. Sheldrick, SHELXS-97, Program for Crystal Structure Determination, University of Göttingen, **1997**.
[88] G. M. Sheldrick, SHELXL-97, Program for Crystal Structure Refinement, University of Göttingen, **1997**.

Received: December 5, 2007
Published online: March 11, 2008

